Molecular basis of growth inhibition by acetate of an adenylate cyclase-deficient mutant of *Corynebacterium glutamicum*

Natalie Wolf[1], Michael Bussmann[1], Abigail Koch-Koerfges[1], Nino Katcharava[1], Julia Schulte[1], Tino Polen[1], Johannes Hartl[2], Julia A. Vorholt[2], Meike Baumgart[1] and Michael Bott[1*]

[1]IBG-1: Biotechnology, Institute of Bio- and Geosciences, Forschungszentrum Jülich, Jülich, Germany

[2]Institute of Microbiology, ETH Zürich, Zürich, Switzerland

***Correspondence:** m.bott@fz-juelich.de

Keywords: *Corynebacterium glutamicum*, cAMP, adenylate cyclase, acetate, uncouplers, membrane potential, GlxR, cytochrome *bc*$_1$-*aa*$_3$ supercomplex

Running title: *Corynebacterium glutamicum* Δ*cyaB* mutant

ABSTRACT

In *Corynebacterium glutamicum*, cyclic adenosine monophosphate (cAMP) serves as an effector of the global transcriptional regulator GlxR. Synthesis of cAMP is catalyzed by the membrane-bound adenylate cyclase CyaB. In this study, we investigated the consequences of decreased intracellular cAMP levels in a Δ*cyaB* mutant. While no growth defect of the Δ*cyaB* strain was observed on glucose, fructose, sucrose, or gluconate alone, the addition of acetate to these growth media resulted in a severe growth inhibition, which could be reversed by plasmid-based *cyaB* expression or by supplementation of the medium with cAMP. The effect was concentration- and pH-dependent, suggesting a link to the uncoupling activity of acetate. In agreement, the Δ*cyaB* mutant had an increased sensitivity to the protonophore carbonyl cyanide *m*-chlorophenyl hydrazone (CCCP). The increased uncoupler sensitivity correlated with a lowered membrane potential of acetate-grown Δ*cyaB* cells compared to wild-type cells. A reduced membrane potential affects major cellular processes, such as ATP synthesis by F_1F_O-ATP synthase and numerous transport processes. The impaired membrane potential of the Δ*cyaB* mutant could be due to a decreased expression of the cytochrome bc_1-aa_3 supercomplex, which is the major contributor of proton-motive force in *C. glutamicum*. Expression of the supercomplex genes was previously reported to be activated by GlxR-cAMP. A suppressor mutant of the Δ*cyaB* strain with improved growth on acetate was isolated, which carried a single mutation in the genome leading to an Ala131Thr exchange in GlxR. Introduction of this point mutation into the original Δ*cyaB* mutant restored the growth defect on acetate. This supported the importance of GlxR for the phenotype of the Δ*cyaB* mutant and, more generally, of the cAMP-GlxR system for the control of energy metabolism in *C. glutamicum*.

INTRODUCTION

The Gram-positive soil bacterium *Corynebacterium glutamicum* was identified as a natural glutamate producer in the 1950s (Kinoshita et al., 1957). Since then, various strains of this bacterium are widely used for the production of amino acids, in particular L–glutamate and L–lysine (Eggeling and Bott, 2015). For several years now, *C. glutamicum* has also been employed in commercial protein production (Freudl, 2017). In addition, strains for the synthesis of numerous other industrially relevant compounds have been developed (Schneider and Wendisch, 2011; Becker and Wittmann, 2012; Wieschalka et al., 2013). The success in rational strain development by metabolic engineering is based on detailed studies of the metabolic and regulatory network of *C. glutamicum* (Eggeling and Bott, 2005; Burkovski, 2008; Yukawa and Inui, 2013). Furthermore, efficient novel technologies for strain development involving high-throughput screening approaches with single-cell metabolite biosensors based on transcriptional regulators have been

established for *C. glutamicum* (Binder et al., 2012; Mustafi et al., 2012; Schendzielorz et al., 2014; Eggeling et al., 2015).

The transcriptional regulator GlxR, a homolog of the cAMP-receptor protein Crp of *Escherichia coli*, is a global regulator of *C. glutamicum* and activates or represses more than 100 genes. Transcriptional regulation by GlxR influences various cellular functions such as central carbon metabolism, respiration, ATP synthesis, or transport processes (Toyoda et al., 2011; Jungwirth et al., 2013). *In vitro,* purified GlxR binds to DNA when complexed with 3',5'-cyclic adenosine monophosphate (cAMP) (Kim et al., 2004; Kohl et al., 2008; Bussmann et al., 2009). Crystal structures of apo- and cAMP-bound GlxR were solved and revealed conformational changes of the homodimer upon cAMP binding (Townsend et al., 2014). GlxR showed negative allosteric behavior, as binding of the first cAMP molecule (K_{D1} = 17 µM) reduced the binding affinity of the second cAMP molecule (K_{D2} = 130 µM) to the structurally identical site in the second monomer (Townsend et al., 2014). The affinity of purified GlxR to a double-stranded oligonucleotide containing a central GlxR consensus binding site increased about 100-fold upon cAMP binding from 8.3 µM to 87 nM (Townsend et al., 2014).

The intracellular cAMP level is determined by the rates of synthesis from ATP via adenylate cyclases (Shenoy et al., 2004), degradation to adenosine monophosphate (AMP) via phosphodiesterases (Richter, 2002), and possibly cAMP export and import processes. In *C. glutamicum*, a single adenylate cyclase was identified, which is encoded by the *cyaB* gene (cg0375) (Kalinowski et al., 2003). CyaB contains an N-terminal membrane-integral domain with six predicted transmembrane helices, which is linked via a HAMP domain to a class IIId catalytic domain (CHD). The HAMP domain might function as transmitter domain, as it was found to have a strong positive stimulatory effect on the adenylate cyclase activity of Rv3645 of *Mycobacterium tuberculosis*, which has the same domain composition as CyaB of *C. glutamicum* (Linder et al., 2004). A *C. glutamicum* mutant lacking about 200 bp of the coding region of the catalytic domain of CyaB (strain CgYA) showed strongly reduced cAMP levels both in glucose minimal medium and LB-acetate medium (Cha et al., 2010). Wild-type cAMP levels could be restored by plasmid-encoded *cyaB*, but not by supplementation of cAMP to the medium. Interestingly, this CgYA mutant had a strong growth defect in acetate and glucose-acetate minimal medium, but not in glucose or ethanol minimal medium (Cha et al., 2010). Since the activities of the glyoxylate cycle enzymes isocitrate lyase and malate synthase were even higher in the mutant than in the wild type (WT) during growth on LB-acetate, the authors speculated that the acetate uptake carrier might play a role in the growth defect of the CgYA mutant (Cha et al. 2010). Degradation of cAMP in *C. glutamicum* is catalyzed by the recently identified phosphodiesterase CpdA (Cg2761) (Schulte et al., 2017b). This enzyme belongs to the class II phosphodiesterases and deletion of the *cpdA* gene

led to an increase of the intracellular cAMP concentration (Schulte et al., 2017b). The Δ*cpdA* mutant exhibited slower growth and a prolonged lag-phase on all tested carbon sources, including glucose, gluconate, citrate, acetate and ethanol (Schulte et al., 2017b). The growth defects could partially be complemented by overexpression of genes that are normally repressed by the cAMP-GlxR complex, such as *ptsI-ptsG* or *citH,* and that are involved in uptake or metabolism of the respective carbon source. This suggested that mainly the higher fraction of cAMP-bound GlxR caused by the increased cAMP level is responsible for the growth defects of the Δ*cpdA* mutant.

The major aim of our current study was to elucidate the molecular basis of the growth inhibition by acetate of a *C. glutamicum* mutant lacking the *cyaB* gene in order to understand the consequences of a reduced cAMP level. Our results suggest that the inhibitory effect of acetate is caused by its property to act as an uncoupler and that a Δ*cyaB* mutant has a reduced capability of generating membrane potential and possibly ATP by oxidative phosphorylation, which might be due to a reduced transcriptional activation of the genes encoding respiratory chain components and the *atp* operon. Support for the assumption that the growth defect of the Δ*cyaB* strain on acetate is due to a reduced activity of GlxR was obtained by the isolation of a suppressor mutant that had lost the growth defect on acetate. This mutant contained a single amino acid exchange in GlxR. In summary, we show that the cAMP level in combination with the global regulator GlxR plays an important role in the bioenergetics of *C. glutamicum*.

MATERIALS AND METHODS

Strains, plasmids and culture conditions

All strains and plasmids used in this study are listed in Table 1. *C. glutamicum* strains were cultivated either in brain heart infusion (BHI) medium (Bacto™ BHI, BD, Heidelberg, Germany) or in CGXII minimal medium (adjusted to pH 7.0 with KOH) supplemented with 3,4-dihydroxybenzoate (30 mg l^{-1}) as iron chelator and different carbon sources (Frunzke et al., 2008) as specified in the results section. For growth experiments, 5 ml BHI medium was inoculated with a single colony and incubated at 30 °C and 130 rpm for 8 h. About 400 µl of this first preculture were used for the inoculation of the second preculture, which was cultivated for about 16 h at 30 °C and 120 rpm in a 100 ml baffled shake flask containing 20 ml CGXII medium with 2% (w/v) glucose. For the main culture, 800 µl CGXII medium in FlowerPlates (m2p-labs, Baesweiler, Germany) was inoculated to an optical density at 600 nm (OD_{600}) of 1 and cultivated in a BioLector microcultivation system (m2p-labs, Baesweiler, Germany) at 1200 rpm, 30 °C and 80% humidity. Growth was followed by measuring the backscatter at 620 nm, which reflects the cell density (Kensy et al., 2009). For cultivations in 500 ml shake flasks, 50 ml CGXII medium was inoculated

with the second preculture to an OD_{600} of 1. The cultivations in shake flasks were performed at 30 °C and 120 rpm and growth was followed by measuring OD_{600}. *E. coli* DH5α was used as host for all cloning purposes and was cultivated at 37 °C in LB medium (Sambrook and Russell, 2001). When required, media were supplemented with kanamycin (25 µg ml^{-1} for *C. glutamicum* and 50 µg ml^{-1} for *E. coli*).

Construction of plasmids and deletion mutants

Plasmids were constructed by standard cloning procedures (Sambrook and Russell, 2001) using the oligonucleotides listed in Table S1. Deletion mutants of *C. glutamicum* were constructed by double homologous recombination as described previously (Niebisch and Bott, 2001). In brief, *C. glutamicum* ATCC 13032 was transformed with the deletion plasmid carrying the up- and downstream regions of the target gene to be deleted. After selection for the first (kanamycin resistance) and second (kanamycin sensitivity, sucrose tolerance) recombination events, Kan^S-Suc^R clones were analyzed by colony PCR and the PCR product of clones carrying the desired deletion was further verified by sequencing.

For construction of a Δ*cyaB* deletion mutant, it had to be considered that the length of the coding region of *cyaB* varies in different annotations, resulting in proteins of either 347 amino acids (MRPVAA…; Cgl0311 of strain ATCC 13032) (Ikeda and Nakagawa, 2003), 547 amino acids (MDTVLE…; Cg0375 of strain ATCC 13032) (Kalinowski et al., 2003), or 501 amino acids (MKWLWG…; cgR_0397 of strain R) (Yukawa et al., 2007). RNAseq analysis of strain ATCC 13032 identified a single transcriptional start site presumably leading to a leaderless *cyaB* mRNA encoding a protein of 508 amino acids (MSRLLR…) (Pfeifer-Sancar et al., 2013). We therefore assumed the latter size to be the correct one, although additional transcriptional start sites and CyaB variants of other length cannot be excluded. For construction of the Δ*cyaB* mutant, we deleted the entire coding region except for the 5'-terminal 37 codons and the 3'-terminal 12 codons including the stop codon. After the second homologous recombination event, nine kanamycin-sensitive and sucrose-resistant clones were analyzed by colony PCR. Four clones harbored the *cyaB* deletion whereas five clones contained the wild-type fragment. Thus, the Δ*cyaB* deletion mutant was obtained without any difficulties.

Isolation of Δ*cyaB* suppressor mutants with improved growth on acetate

The acetate-sensitive Δ*cyaB* strain was cultivated in CGXII medium with 150 mM potassium acetate as sole carbon source. The culture was prepared as described above. To obtain acetate-tolerant suppressor clones, cultivations were performed for at least 90 h in a BioLector. Cultures that started to grow and reached comparable backscatter values as the WT were streaked out on

BHI agar plates and single colonies were inoculated again in CGXII medium with 150 mM potassium acetate. Cultures that grew better than the Δ*cyaB* parental strain were streaked out again on BHI agar plates. The genomic DNA of such clones was isolated and used for whole genome sequencing.

Genomic DNA sequencing

DNA of the samples was purified with the DNeasy Blood and Tissue kit (Qiagen, Hilden, Germany) starting with the "pretreatment of Gram-positive bacteria", as described in the manufacturer's instructions. The obtained DNA was dried and resuspended in max. 100 µl ddH_2O. For library preparation, the NEBNext Ultra II DNA Library Prep kit for Illumina (New England Biolabs GmbH, Frankfurt am Main, Germany) was used with 2 µg genomic DNA of each sample following the manufacturer's instructions. The resulting indexed libraries were quantified using the KAPA Library Quantification kit (Peqlab, Bonn, Germany) and normalized for pooling. Sequencing was performed on a MiSeq instrument (Illumina, San Diego, USA) using paired-end sequencing with a read-length of 2 × 150 bp. Data analysis and base calling were accomplished with the CLC Genomics workbench (Qiagen, Hilden, Germany). Reads of the parental Δ*cyaB* strain and the suppressor strains were mapped to the genome sequence BA000036.3 of *C. glutamicum* ATCC 13032 (Ikeda and Nakagawa, 2003).

Determination of mRNA levels by quantitative real-time PCR (qRT-PCR)

For quantifying the mRNA levels of *ctaD*, *ctaC*, and *qcrC* in *C. glutamicum* WT and the Δ*cyaB* mutant, RT-PCR was performed. Therefore, cells were grown in CGXII medium containing a glucose-acetate mixture (100 mM each) and harvested at an OD_{600} of 6. Cells were disrupted by the addition of QIAzol Lysis Reagent (Qiagen, Hilden, Germany) followed by bead beating with a Precellys24 device (Peqlab Biotechnologie, Erlangen, Germany). RNA was purified and concentrated with an RNeasy Mini kit (Qiagen, Hilden, Germany) including a DNase I treatment. Reverse transcription of total RNA samples to cDNA was performed using Superscript™ III reverse transcriptase and random primers (Invitrogen, Carlsbad, USA) following the manufacturer's instructions. For the quantitative real-time PCR, KAPA SYBR® FAST qPCR Master Mix (2x) (Roche, Basel, Switzerland) was used following the manufacturer's protocol. Primer pairs used for the reactions are listed in Table S1. As reference gene *hpt* (cg2985) was used with the oligonucleotides listed in Table S1. Fluorescence measurements and analysis of the results were conducted using a qTower 2.2 and the software qPCR-soft 3.1 (Analytic Jena, Jena, Germany). RNA was isolated from three independent cultures of each strain (biological triplicates) and for each sample technical duplicates were performed.

193

194 **Global gene expression analysis using DNA microarrays**

195 Preparation of RNA and synthesis of fluorescently labelled cDNA were carried out as described
196 (Möker et al., 2004). Custom-made DNA microarrays for *C. glutamicum* ATCC 13032 printed with
197 70mer oligonucleotides were obtained from Operon (Cologne, Germany) and are based on the
198 genome sequence entry NC_006958 (Kalinowski et al., 2003). Hybridization and stringent washing
199 of the microarrays were performed according to the instructions of the supplier. Processed and
200 normalized data as well as experimental details (Brazma et al., 2001) were stored in the in-house
201 microarray database for further analysis (Polen and Wendisch, 2004). Using the DNA microarray
202 technology, the genome-wide mRNA concentrations of *C. glutamicum* wild type were compared
203 with those of the mutant strain *C. glutamicum* Δ*cyaB*. The strains were cultivated in CGXII medium
204 with a glucose-acetate mixture (100 mM each). RNA used for the synthesis of labelled cDNA was
205 prepared from cells in the exponential growth phase. Three independent DNA microarray
206 experiments were performed, each starting from independent cultures.

207

208 **Determination of cAMP**

209 Cell extracts were prepared as described previously (Schulte et al., 2017b) and the cAMP
210 concentration was measured without dilution with the direct cAMP ELISA kit (Enzo Life Sciences
211 GmbH, Lörrach, Germany) following the manufacturer's instructions. Amounts of cAMP were
212 related to the protein content of the supernatant of the cell extract. The product specification of the
213 used cAMP ELISA kit (Direct cAMP ELISA kit; Enzo, Lausen, Switzerland) reports the following
214 cross-reactivities with nucleotides other than cAMP, which is set as 100%: AMP, 0.33%; ATP,
215 0.12%; cyclic GMP, GMP, GTP, cyclic UMP, CTP, all <0.001%. For determining the cross-
216 reactivities, the nucleotides were dissolved in assay buffer to a concentration of 2000 pmol/ml,
217 which is 10-fold higher than the highest concentration used for cAMP in the non-acetylated variant
218 of the assay. The apparent concentrations determined for the non-cAMP nucleotides, e.g. 6.6
219 pmol/ml for AMP, was divided by the real AMP concentration in the assay (2000 pmol/ml) and
220 multiplied with 100 to give the cross-reactivity in %.

221 Additionally, intracellular cAMP was measured by LC-MS/MS. *C. glutamicum* cells were
222 grown to the exponential phase (OD_{600} of ~5). For the sampling, cells from a culture volume
223 corresponding to 4 ml of OD_{600} of 1 were harvested. Sampling, quenching, metabolite extraction
224 and measurements were performed as previously described (Müller et al., 2015; Hartl et al., 2017).
225 Briefly, metabolite separation was achieved by reverse-phase-ion-pairing (tributylamin) liquid
226 chromatography using a nLC-ultra (Eksigent) system. The LC was hyphenated to a QExactive Plus
227 Orbitrap (Thermo Fisher) mass spectrometer with an electrospray ionization probe. The MS was

operating in negative mode; the resolution was set to 70 000 (at m/z 200). cAMP was measured using parent reaction monitoring (PRM) with m/z 328.045 as the precursor ion and quantified with the corresponding m/z 134.0465 fragment. Fragmentation was achieved by higher energy collisional dissociations (HCDs) with a normalized collision energy (NCE) of 30.0. cAMP was identified by exact mass (m/z tolerance of 0.003 Da) as well as matching retention time and fragmentation pattern with an analytical 3',5'-cAMP standard. cAMP was quantified by peak integration using the trapezoid rule; absolute quantification was performed by external calibration. The calibration curve of reference solutions with known cAMP concentrations was fitted by linear regression. The intracellular cAMP concentrations in *Corynebacterium* were estimated assuming a correlation factor of 250 mg cell dry weight (CDW) l^{-1} at OD_{600} of 1 (Kabus et al., 2007) and a corresponding intracellular volume of 1.44 µl per mg CDW (da Luz et al., 2016). The limit of detection (LOD) was estimated to be 14 amol l^{-1} by calculating 3.3 standard deviations of the y-intercepts divided by the slope obtained from linear regression (ICH, 2005) of reference cAMP solutions; the LOD was confirmed by visual inspection. Assuming similar dilution factors as for measured *Corynebacterium* extracts, this corresponds to an LOD of ~0.1 µmol l^{-1} from cell extracts.

Measurement of membrane potential via flow cytometry

The membrane potential of *C. glutamicum* cells was determined by flow cytometry using the fluorescent dye 3,3′-diethyloxacarbocyanine iodide (DiOC2(3)) (Novo et al., 1999; Novo et al., 2000). The assay was performed according to a previously established protocol for *C. glutamicum* (Neumeyer et al., 2013). In brief, the strains were cultivated in baffled shake flasks with 50 ml CGXII medium containing either 100 mM glucose, or 100 mM acetate, or 200 mM acetate (precultures as described for the BioLector cultivation). Measurement of the membrane potential was performed when cells had reached the mid-exponential growth phase (OD_{600} of ~ 5). The culture was diluted with FACSFlow™ buffer to an OD_{600} of 0.05 and cells were stained for 30 min with 30 µM DiOC2(3) (3 mM stock solution in dimethyl sulphoxide, Sigma-Aldrich, Germany) and analyzed using a FACS Aria II and BD Diva software (BD Biosciences, Heidelberg, Germany). Green fluorescence was measured at an excitation wavelength of 488 nm and an emission wavelength of 497 nm, red fluorescence at an excitation wavelength of 488 nm and an emission wavelength of 610 nm. For each sample, 100,000 cells were measured at 2000 cells s^{-1}. The red/green fluorescence ratio was analyzed using FlowJo V.10 software and plotted as a histogram with GraphPad Prism8.

Quantitative determinations of carbon sources

Glucose, gluconate and acetate concentrations in culture supernatants were determined as described (Koch-Koerfges et al., 2012) by ion-exchange chromatography using an Agilent 1100 HPLC system (Agilent Technologies, Waldbronn, Germany) equipped with a cation exchange column (Organic Acid Resin 300 x 8 mm, CS Chromatographie Service, Langerwehe, Germany). Isocratic elution within 40 min with 100 mM H_2SO_4 and a flow rate of 0.4 ml/min at 40 °C was used. Organic acids were detected using a diode array detector at 215 nm and glucose was analyzed by a refraction index (RI) detector in the same run. The quantification of organic acids and glucose was based on a calibration curve with external standards.

TMPD enzyme assay

N,*N*,*N*',*N*'-tetramethyl-*p*-phenylenediamine (TMPD) oxidase activity was measured spectrophotometrically at 562 nm in a 96-well plate with an Infinite M1000 PRO microplate reader (Tecan, Männedorf, Switzerland). TMPD was added to 100 mM Tris-HCl buffer pH 7.5 containing isolated membrane protein to a final concentration of 200 µM. For the calculation of the TMPD oxidation rate, an extinction coefficient of 10.5 mM^{-1} cm^{-1} was used (Sakamoto et al., 2001). The autooxidation rate of TMPD was recorded using samples containing only buffer and 200 µM TMPD and subtracted from the rates of the membranes. The cells for these measurements were cultivated at 30°C and 90 rpm in 5 l baffled shake flasks with 500 ml CGXII medium and glucose plus acetate (each 100 mM) as carbon source. The cultures were harvested in the exponential growth phase at the OD_{600} of 10. The preparation of cell membranes was performed as described (Niebisch and Bott, 2003).

Electrophoretic mobility shift assays (EMSAs) with purified GlxR

EMSAs were performed to compare *in vitro* binding of the wild-type GlxR protein ($GlxR_{WT}$) and the variant $GlxR_{A131T}$ to selected DNA target sites. The gene *glxR* was amplified from genomic DNA of *C. glutamicum* WT with the oligonucleotides GlxR-twin1 and GlxR-twin2. A DNA fragment with a Twin-Strep tag-encoding sequence was amplified with the oligonucleotides GlxR-twin3 and GlxR-twin4 using a suitable plasmid with the corresponding sequence as template. Gibson assembly was performed with pAN6 cut with NdeI and NheI, the glxR fragment and the Twinstrep-tag fragment resulting in the plasmidpAN6-*glxR*-Twinstrep. The oligonucleotides GlxR-A131T_fw and GlxR-A131T_rv were used to introduce the mutation leading to the amino acid exchange A131T in GlxR using the QuickChange Site-Directed Mutagenesis Kit (Agilent, Waldbronn, Germany). The resulting plasmid was named pAN6-*glxR*-A131T-Twinstrep. Overproduction of $GlxR_{WT}$ or $GlxR_{A131T}$ was performed by cultivation *E.coli* BL21(DE3) transformed with pAN6-*glxR*-Twinstrep or pAN6-*glxR*-A131T-Twinstrep in ZYM-5052 auto-

induction medium (Studier, 2005). After harvesting and disrupting the cells, proteins were purified using Strep-Tactin XT affinity chromatography according to the protocol of the supplier (IBA Life Sciences, Göttingen, Germany). Subsequently, the protein were further purified by size exclusion chromatography using a Superdex 200 increase column using a buffer composed of 100 mM Tris-HCl pH 7.5, 5% (v/v) glycerol, 100 mM KCl, 20 mM $MgCl_2$, and 1 mM EDTA.

EMSAs were performed as described previously (Bussmann et al., 2009) using the following DNA fragments: (i) a 140 bp DNA fragment upstream of *ctaD* extending from -127 to -261 upstream of the *ctaD* start codon; (ii) a 132 bp DNA fragment upstream of *ctaCF* extending from -102 to -234 upstream of the *ctaC* start codon; (iii) a 136 bp DNA fragment covering an intragenic region of the gene cg3153. The former two DNA fragments contain previously described GlxR binding sites (Kohl et al., 2008; Toyoda et al., 2011). The respective DNA fragments were generated by PCR and purified with the DNA Clean & Concentrator Kit (Zymo Research, Freiburg, Germany).

RESULTS AND DISCUSSION

cAMP levels in *C. glutamicum* WT and mutants lacking *cyaB* or *cpdA*

In order to confirm previous studies with the *C. glutamicum* mutant strain CgYA lacking approximately 200 bp coding region of the catalytic domain of the adenylate cyclase CyaB (Cha et al., 2010), we constructed another Δ*cyaB* mutant lacking the entire coding region (see Materials and Methods). The cAMP level of this mutant was compared with that of the WT and the Δ*cpdA* mutant lacking the cAMP phosphodiesterase (Schulte et al., 2017b) using an enzyme-linked immunosorbent assay (ELISA). The strains were grown in CGXII glucose medium to an OD_{600} of about 5 (exponential growth phase). As shown in Table 2, the cAMP level of the Δ*cyaB* mutant (~20 pmol (mg protein)$^{-1}$) amounts to only 20% of the cAMP level of the WT (~100 pmol (mg protein)$^{-1}$), whereas that of the Δ*cpdA* mutant was higher (~144 pmol (mg protein)$^{-1}$). These results confirmed that the lack of the adenylate cyclase CyaB causes a strong decrease of the cAMP level, which is in agreement with previous results (Cha et al., 2010; Toyoda et al., 2011; Schulte et al., 2017b). It should be noted that the absolute values obtained in the ELISA measurements published in these studies differ significantly.

As described above, bioinformatic analysis revealed only a single adenylate cyclase-encoding gene (*cyaB*) in the genome of *C. glutamicum*. Therefore, deletion of *cyaB* should result in the complete lack of the cAMP. However, both in our Δ*cyaB* mutant as well as in previously analyzed *cyaB* mutants of strain ATCC 13032 (Cha et al., 2010) and strain R (Toyoda et al., 2011) a residual cAMP level was measured by ELISA assays, raising the question for the source of this residual

cAMP. The kit used in this study (Enzo Life Sciences GmbH, Lörrach, Germany) shows low cross-reactivity to AMP and ATP, which might contribute to the residual signal in the Δ*cyaB* mutant. Alternatively or additionally, *C. glutamicum* might possess another enzyme with adenylate cyclase activity besides CyaB, which contributes to the residual cAMP level in the Δ*cyaB* mutants and which is not detectable in bioinformatic searches using members of the known classes of adenylate cyclases (Shenoy et al., 2004). If a yet unknown novel enzyme with adenylate cyclase activity exists in *C. glutamicum*, a deletion of the *cpdA* gene in the Δ*cyaB* background might lead to an increase of cAMP. Therefore, we constructed a Δ*cyaB*Δ*cpdA* double mutant and determined the cAMP level by the ELISA kit. Although a small increase was detected for the double mutant, the difference to the Δ*cyaB* mutant was not significant (Table 2). In growth experiments with glucose or acetate minimal medium, the Δ*cyaB*Δ*cpdA* mutant behaved like the Δ*cyaB* mutant (Fig. S1), arguing against the existence of an alternative adenylate cyclase besides CyaB.

As the ELISA-based assay might be influenced by cross-reacting metabolites, LC-MS/MS was applied as an alternative method to quantify cAMP levels. With this method, we determined an absolute concentration of cAMP of ~1 µM in wild-type cells, whereas a ~3.5-fold higher concentration was determined in the Δ*cpdA* mutant. cAMP was not detected in the Δ*cyaB* mutant and in the Δ*cyaB*Δ*cpdA* double mutant. These results support the possibility that the residual cAMP levels determined by the ELISA assay in the latter two mutants might be caused by cross-reactivities and suggest that CyaB is the only adenylate cyclase present in *C. glutamicum*.

Sensitivity of the Δ*cyaB* mutant to acetate

Growth of the Δ*cyaB* mutant and the WT with different carbon sources was compared using the BioLector cultivation system. In CGXII minimal medium containing 100 mM of either glucose, gluconate, fructose, or sucrose as carbon source, the Δ*cyaB* mutant grew like the WT, whereas a clear growth defect was observed for the mutant when 100 mM acetate served as carbon source (Fig. 1). In media containing mixtures of gluconate and acetate, glucose and acetate, fructose and acetate, or sucrose and acetate (100 mM of each carbon source), the Δ*cyaB* mutant showed a strong growth defect, whereas the WT was unaffected and grew to higher cell densities (measured as higher backscatter values) (Fig. 1). The data obtained with the Δ*cyaB* mutant for glucose, acetate, and the glucose-acetate mixture are in agreement with those described previously for the CgYA mutant, whereas the results for fructose-acetate and sucrose-acetate disagree, as growth of the CgYA mutant on these mixtures was reported not to be impaired (Cha et al., 2010). Our results indicate that acetate inhibits growth of the Δ*cyaB* mutant irrespective of the presence of an additional carbon source.

With respect to the inhibitory effect of acetate, ethanol is a particularly interesting carbon source, as its catabolism in *C. glutamicum* involves acetate as an intermediate. Ethanol degradation proceeds via the initial oxidation to acetaldehyde by alcohol dehydrogenase followed by a second oxidation to acetate by acetaldehyde dehydrogenase (Arndt and Eikmanns, 2007; Arndt et al., 2008). Acetate is then converted via acetyl phosphate to acetyl-CoA by acetate kinase and phosphotransacetylase and acetyl-CoA is oxidized in the TCA cycle with the glyoxylate cycle serving as an anaplerotic reaction (Wendisch et al., 2000; Gerstmeir et al., 2003; Bott, 2007). As shown in Fig. S2, the Δ*cyaB* mutant grew like the WT in CGXII medium containing 150 mM ethanol as carbon source. This result is in agreement with data reported previously for the CgYA mutant (Cha et al., 2010) and shows that acetate degradation is functional in the Δ*cyaB* mutant.

Growth of the WT and the Δ*cyaB* mutant was also compared in shake flasks in order to be able to follow the consumption of the carbon sources during cultivation (Fig. 2). The growth defect of the Δ*cyaB* mutant during growth on a glucose-acetate mixture (100 mM each) was confirmed and resulted in a retarded consumption of both carbon sources compared to the WT. In CGXII medium containing a gluconate-acetate mixture, the Δ*cyaB* mutant also showed a growth defect and retarded consumption of gluconate and acetate compared to the WT. In contrast to glucose, fructose, and sucrose, gluconate is not taken up via the PEP-dependent phosphotransferase system (PTS), but via the secondary transporter GntP (Frunzke et al. 2008). The fact that acetate was completely consumed confirms that acetate catabolism is functional in the Δ*cyaB* mutant.

Abolishment of the growth defect of the Δ*cyaB* mutant in the presence of acetate

The Δ*cyaB* mutant and the WT were transformed with the *cyaB* expression plasmid pAN6-*cyaB* or the parent vector pAN6. As shown in Fig. 3, the growth defect of the Δ*cyaB* mutant in glucose-acetate medium was abolished by plasmid-based expression of *cyaB*, but not by the presence of the vector alone. This result confirmed that the *cyaB* deletion rather than a hypothetical secondary mutation that might have occurred during mutant construction was responsible for the acetate sensitivity. In a previous study we showed that cAMP addition to the medium influences GlxR-based gene expression, indicating that it can enter the cell (Schulte et al., 2017a). We therefore tested the influence of cAMP addition on growth of the Δ*cyaB* mutant and could show that 10 mM cAMP abrogated the growth defect in the presence of acetate, confirming that it is due to a lowered cAMP level (Fig. 3). In the case of the CgYA mutant, addition of cAMP to the medium could not reverse the growth inhibition (Cha et al., 2010). The reason for this discrepancy is unknown. Uptake of 3',5'-cAMP was previously reported for *E. coli* and marine bacteria, but no distinct transporter could be identified (Saier et al., 1975; Goldenbaum and Hall, 1979; Ammerman and Azam, 1982).

401

402 **Concentration and pH dependency of growth inhibition of the Δ*cyaB* mutant by acetate**

403 As described above, the inhibitory effect of acetateon growth of the Δ*cyaB* mutant was independent
404 of the presence of additional carbon sources. The difference when comparing growth on ethanol
405 and growth on acetate is that during ethanol degradation acetate is only a metabolic intermediate
406 that does not accumulate to high concentrations but is directly catabolized. In contrast, when acetate
407 is used as carbon source, it is present in a high concentration outside of the cell. It was speculated
408 that inhibition of acetate uptake by the secondary monocarboxylate transporter MctC (Cg0953)
409 might play a role for the growth defect (Cha et al., 2010). However, under the conditions used in
410 our studies (100 mM acetate, pH 7), uptake of acetate by passive diffusion is completely sufficient,
411 as shown by the fact that growth of a *mctC* deletion mutant on acetate at pH 7 was unaffected
412 (Jolkver et al., 2009).

413 Based on the above considerations, we assumed that the inhibitory effect of acetate on growth
414 of the Δ*cyaB* mutant is due to its property to act as an uncoupler (Axe and Bailey, 1995; Pinhal et
415 al., 2019). We tested whether the inhibitory effect of acetate is concentration- and pH-dependent.
416 Weak acids such as acetate become more effective as proton translocator when the pH gets closer
417 to their pK_a (4.76 in the case of acetic acid). In a first set of experiments, the WT and the Δ*cyaB*
418 mutant were grown in CGXII medium containing 100 mM, 150 mM, or 200 mM acetate. In the
419 case of the WT, increased acetate concentrations led to increased cell densities, but did not affect
420 the growth rate strongly. In contrast, growth inhibition of the Δ*cyaB* mutant clearly correlated with
421 increasing acetate concentrations (Fig. 4A). The dose-dependent negative impact of acetate on
422 growth of the Δ*cyaB* mutant was also observed in cultivations in CGXII medium with 100 mM
423 glucose and either 50 mM or 100 mM acetate (Fig. S3). Furthermore, the inhibitory effect of acetate
424 was observed independent of whether sodium acetate or potassium acetate were used for
425 preparation of the media, showing that this effect is not caused by the cation (data not shown). For
426 testing the pH dependency of growth inhibition by acetate, the MOPS buffer of the standard CGXII
427 medium was substituted by a mixture of 20 g l^{-1} MOPS (pK_a 7.20) and 20 g l^{-1} MES (pK_a 6.15) and
428 pH values of 6.0, 6.5, and 7.0 were adjusted by addition of KOH or HCl. Besides media with
429 100 mM acetate, also media with 100 mM glucose were used at the indicated pH values. As shown
430 in Fig. 4B, growth of the WT and the Δ*cyaB* mutant in glucose medium was comparable and hardly
431 affected by the initial pH value. In contrast, growth of the mutant in acetate medium was strongly
432 affected by the pH, showing almost no growth at pH 6.5 and pH 6.0 (Fig. 4C). In summary, the
433 inhibitory effect of acetate on growth of the Δ*cyaB* mutant was both concentration- and pH-
434 dependent, supporting our assumption that it is due to the uncoupling properties of acetate.

435

Uncoupler sensitivity and membrane potential of WT and the Δ*cyaB* mutant

The results described above suggested that the Δ*cyaB* mutant is more sensitive to uncouplers than the WT. To further confirm this assumption, the influence of the protonophore carbonyl cyanide *m*-chlorophenyl hydrazone (CCCP) (Heytler and Prichard, 1962) on growth in CGXII medium with glucose was tested (Fig. 5A and B). The Δ*cyaB* mutant was more sensitive to CCCP than the WT. In the presence of 5 µM CCCP, the mutant was stronger inhibited than the WT. In the presence of 10 µM CCCP, the mutant was not able to grow any more, while the WT showed residual growth. At 15 µM CCCP, neither strain was able to grow.

The increased sensitivity to acetate and CCCP of the Δ*cyaB* mutant compared to the WT might be due to a reduced capability of the mutant to build up pmf, which is composed of the membrane potential Δψ and the pH gradient ΔpH ((Nicholls and Ferguson, 2002). At pH 7, the pmf of *C. glutamicum* WT is about 200 mV and formed almost exclusively by the membrane potential of 180 mV (Follmann et al., 2009; Koch-Koerfges et al., 2012). We compared Δψ of the WT and the Δ*cyaB* mutant using the dye 3,3′-diethyloxacarbocyanine iodide (DiOC2(3)), which exhibits green fluorescence in all stained bacteria and shifts towards red emission due to self-association of dye molecules in dependency of Δψ. Higher Δψ correlates with increased red fluorescence and the ratio of red/green fluorescence gives a relative measure of the membrane potential (Novo et al., 1999; Novo et al., 2000). This method does not give absolute values for the membrane potential but is useful for relative comparison of the membrane potential of different strains.

Using a previously established protocol (Neumeyer et al., 2013) we first confirmed that treatment of wild-type cells grown in CGXII glucose medium with 50 µM CCCP led to the expected decrease of the red/green fluorescence ratio indicating a collapsed or strongly reduced Δψ (Fig. 5C, panel I). When cells of the WT and the Δ*cyaB* mutant cultivated in glucose medium to the exponential growth phase were analyzed, no significant difference red/green ratio was observed, indicating that both cells had a comparably high Δψ (Fig. 5C, panel II). The histograms differed, however, when the cells were cultivated in CGXII medium with 100 mM acetate as carbon source. In this case, the mean fluorescence ratio of wild-type cells was almost unaltered, whereas that of the Δ*cyaB* mutant was strongly decreased (Fig. 5C, panel III). This shift of the red/green ratio indicates that the membrane potential of the Δ*cyaB* mutant is reduced compared to the membrane potential of the WT. For wild-type cells cultivated with 200 mM acetate, the mean fluorescence ratio was reduced compared to cells grown with glucose or 100 mM acetate, in line with the concentration-dependent uncoupling effect of acetate, but the ratio of the Δ*cyaB* mutant was much stronger affected (Fig. 5C, panel IV). These results indicate that acetate affects Δψ of the Δ*cyaB* mutant much more strongly than Δψ of the WT.

Role of the cytochrome *bc*$_1$-*aa*$_3$ supercomplex for acetate sensitivity

The results described above suggest that the cAMP deficiency of the Δ*cyaB* mutant causes a reduced ability to maintain a high membrane potential in the presence of the uncoupler acetate. In *C. glutamicum* cultivated under oxic conditions, pmf is generated by the cytochrome *bc*$_1$-*aa*$_3$ supercomplex (6 H^+/2 e^-) and by cytochrome *bd* oxidase (2 H^+/2 e^-) (Bott and Niebisch, 2003; Niebisch and Bott, 2003; Kabashima et al., 2009). We previously showed that Δψ is reduced in a Δ*qcr* mutant lacking a functional supercomplex, wheras it is comparable to the WT in a Δ*cydAB* mutant lacking cytochrome *bd* oxidase (Koch-Koerfges et al., 2013). Therefore, a link between the cAMP level and the activity of the respiratory supercomplex might exist.

The transcriptional regulator GlxR is the only protein currently known in *C. glutamicum* whose activity is controlled by the cAMP level. In the presence of cAMP, purified GlxR was shown to bind to oligonucleotides covering predicted GlxR-binding sites in the promoter regions of the *ctaCF* operon, the *ctaE-qcrCAB* operon, and *ctaD*, which encode the subunits of the cytochrome *bc*$_1$-*aa*$_3$ supercomplex (Kohl et al., 2008). In glucose-grown cells of strain R, chromatin affinity chromatography followed by DNA chip analysis of the enriched DNA fragments (ChIP-chip) confirmed that Strep-tagged GlxR binds *in vivo* to these proposed binding sites (Toyoda et al., 2011). Mutation of the GlxR-binding sites in the *ctaC* and *ctaD* promoter regions of genomically integrated single-copy transcriptional fusions reduced expression of the reporter gene *lacZ* in yeast extract-containing medium with either glucose or acetate by about 15 – 40% (Toyoda et al., 2011). These results indicated that GlxR acts as a transcriptional activator of the genes encoding the cytochrome *bc*$_1$-*aa*$_3$ supercomplex. The reduced cAMP level in the Δ*cyaB* mutant might thus cause a reduced expression of the genes for the *bc*$_1$-*aa*$_3$ supercomplex leading to a reduced capacity to build up membrane potential and to counteract the uncoupling activity of acetate. A transcriptome comparison of the Δ*cyaB* mutant with the WT revealed reduced expression of all genes encoding the supercomplex (Table S2). Additionally, we also performed qRT-PCR of *ctaC*, *ctaD*, and *qcrC* and the resulting data also showed decreased expression of these genes in Δ*cyaB* mutant (Table S2).

To test for differences of cytochrome *aa*$_3$ activity in the Δ*cyaB* mutant and the WT, the TMPD oxidase activity of membrane fractions of the two strains grown in CGXII medium with glucose-acetate was determined. TMPD is supposed to donate electrons to cytochrome c_1. The TMPD oxidase activity of the Δ*cyaB* mutant was 35% reduced (280 ± 11 nmol TMPD oxidized min^{-1} (mg membrane protein)$^{-1}$) compared to the WT (433 ± 22 nmol TMPD oxidized min^{-1} (mg membrane protein)$^{-1}$), supporting the assumption that a reduced activity of the *bc*$_1$-*aa*$_3$ supercomplex contributes to the uncoupler sensitivity of the mutant during growth on acetate.

To further support the relevance of the cytochrome bc_1-aa_3 supercomplex for the acetate sensitivity of the Δ*cyaB* mutant, growth of the WT and the Δ*qcr* mutant was compared in CGXII medium with glucose, glucose plus acetate, or acetate (Fig. 6). Already in glucose medium the Δ*qcr* mutant showed a growth defect, as known from previous studies (Niebisch and Bott, 2001). In medium with glucose and acetate, the growth defect of the Δ*qcr* mutant became more severe, whereas in minimal medium with acetate as sole carbon source the Δ*qcr* mutant showed no growth. These results support the assumption that the cytochrome bc_1-aa_3 branch of the respiratory chain is crucial for growth on acetate.

Growth on acetate does not allow net ATP synthesis by substrate level phosphorylation and is strictly dependent on oxidative phosphorylation by F_1F_O-ATP synthase (Koch-Koerfges et al., 2012). Interestingly, also the expression of the *atpBEFHAGDC* operon (cg1362-cg1369) encoding the eight subunits of F_1F_O-ATP synthase was shown to be activated by GlxR (Toyoda et al., 2011) and therefore might be lowered in the Δ*cyaB* mutant. The transcriptome comparison supported this assumption with about 2-fold lowered mRNA levels of the *atp* genes in the Δ*cyaB* mutant. Consequently, the growth defect of the mutant on acetate is most likely additionally caused by a reduced ATP synthesis via oxidative phosphorylation, caused by reduced synthesis of the bc_1-aa_3 supercomplex and F_1F_O-ATP synthase.

Isolation of suppressor mutants of the Δ*cyaB* strain with improved growth on acetate

To get further insights into the molecular basis of the acetate sensitivity of the Δ*cyaB* mutant, we isolated Δ*cyaB* suppressor mutants that show improved growth on acetate. As shown in Fig. S4A, three independent cultures started to grow after about 80 h of incubation in acetate minimal medium. After plating on BHI agar plates, single colonies were picked from each of the three cultures and tested again for growth on acetate. As shown in Fig. S4B, two of the suppressor mutants named Δ*cyaB*_sup1 and Δ*cyaB*_sup3 grew almost like the WT, whereas the third one Δ*cyaB*_sup2 showed slower growth than the other two mutants. Genomic DNA of the three suppressor mutants was isolated and sequenced with average coverages of 82, 81, and 106 for Δ*cyaB* _sup1, Δ*cyaB* _sup2, and Δ*cyaB* _sup3, respectively. For strain Δ*cyaB*_sup1 a single point mutation was identified compared to the parent Δ*cyaB* mutant at position 307072 (numbering according to BA000036.3), which is located in the *glxR* gene and leads to an Ala131Thr exchange. The frequency of the mutation in the Δ*cyaB*_sup1 mutant was 100%. Interestingly, the same mutation was also identified in strain Δ*cyaB*_sup3, which additionally carried a second point mutation at position 2564086 (frequency 97.0%) leading to a silent mutation in codon 106 (Gly) of the ribose 5-phosphate isomerase gene *rpi* (cg2658). The suppressor mutant Δ*cyaB*_sup2 did not

carry a mutation in *glxR*, but two point mutations in intergenic regions, one between promoters P1 and P2 of *gltA* (cg0949; citrate synthase) (van Ooyen et al., 2011) at position 877553 (A to G, frequency 100%) and the other one 39 bp upstream of the start codon of cg1660 encoding a putative manganese efflux pump (position 1548741, G to C, frequency 100%). The position of the point mutation in the *gltA* promoter does not overlap with known regulator binding sites for RamA and GlxR (van Ooyen et al., 2011) and therefore the effect of this mutation cannot be predicted. Similarly, the effect of the second mutation upstream of cg1660 cannot be deduced as neither the promoter nor the regulation of this gene is known.

The finding that two of the three independently obtained suppressor mutants carried the same mutation (A131T) in GlxR supports the crucial role of this regulator for the acetate sensitivity of the Δ*cyaB* mutant. To confirm that this mutation can rescue the acetate sensitivity of the Δ*cyaB* strain, it was introduced by site-directed mutagenesis into the genome of the Δ*cyaB* mutant and for comparison into the WT. The resulting strains Δ*cyaB*::*glxR*_A131T and WT::*glxR*_A131T showed comparable growth in minimal medium with glucose compared to the parental strains Δ*cyaB* and the WT (Fig. S4C). Importantly, the Δ*cyaB*::*glxR*_A131T strain showed wild-type like growth in acetate minimal medium, confirming the phenotype of strain Δ*cyaB* _sup1 (Fig. S4D).

The alanine residue at position 131 of GlxR is highly conserved in homologs from other *Corynebacterium* species and *Mycobacterium tuberculosis* as well as in CRP of *E. coli* (Fig. S4E). Ala131 is located in the central α-helix of GlxR, which forms the dimer interface, and is positioned close to important cAMP-binding residues (Townsend et al., 2014) (Fig. S4E and G). Overlays of the crystal structures of apo- and holo-GlxR and of models with the Ala131T exchange are shown in Fig. S4F and G. The mutation apparently does not lead to large structural changes, making it difficult to predict the functional consequences of the amino acid exchange. Due to the vicinity of residue 131 to the cAMP-binding site, the A131T exchange might have altered the influence of cAMP on DNA-binding. We therefore tested whether purified GlxR-A131T still requires cAMP for binding to DNA targets in electrophoretic mobility shift assays. As shown in Fig. S5, binding of GlxR-A131T to DNA fragments covering the GlxR-binding sites in front of *ctaD* and *ctaC* was still dependent on cAMP. However, the *in vivo* situation is probably different. ChIP-Chip experiments with a *cyaB*-deletion strain of *C. glutamicum* R clearly showed GlxR-binding to target sites despite the lack of CyaB, although with decreased affinity (Toyoda et al., 2011).

The most intensively studied homolog of GlxR is CRP of *E. coli*. Many studies were performed in which *E. coli* Δ*cya* strains were used to select for mutants that regained the ability to grow on carbon sources like lactose, maltose, or xylose requiring activation of gene expression by CRP. These studies have recently been summarized (Frendorf et al., 2019) and led the authors to conclude that adaptive mutations occur predominantly in the cAMP binding site, the D-α-helix, and

574 in the RNA polymerase activating domains AR1 and AR2, which likely affect ligand binding,
575 ligand-induced allosteric transitions, or the productive interaction with the core RNA polymerase,
576 respectively. In these studies, no mutation was found in CRP residue A121, which corresponds to
577 A131 of GlxR. However, it has to be considered that although the 3-dimensional fold of GlxR and
578 CRP is very similar, the structural changes observed for GlxR upon cAMP binding are quite distinct
579 from those observed for CRP (Townsend et al., 2014). It was concluded that the mechanisms of
580 allosteric binding and activation of DNA-binding differ considerably in the CRP/FNR family
581 without dramatic structural changes and that the same 3-dimensional fold is finetuned using small
582 structural changes coupled with changes in dynamic behavior to achieve the optimal combination
583 of allostery and DNA recognition (Townsend et al., 2014). This situation makes a prediction of the
584 effects of the A131T mutation in GlxR based on studies of *E. coli* CRP virtually impossible.
585
586 **Conclusions**
587 The aim of this study was to elucidate the consequences of a reduced cAMP level in *C. glutamicum*
588 caused by the lack of the adenylate cyclase CyaB and in particular the inhibitory effect of acetate
589 on growth of the Δ*cyaB* mutant. Our results strongly suggest that this effect is mainly caused by the
590 uncoupling activity of acetate, as it is concentration- and pH-dependent and occurs also in the
591 presence of an additional carbon source such as glucose, fructose, sucrose, or gluconate. Evidence
592 was obtained that the Δ*cyaB* mutant has a lower $\Delta\psi$ on acetate than the WT, suggesting a reduced
593 capability to build up pmf. As the growth defect of the Δ*cyaB* mutant could be rescued by
594 supplementation of the medium with cAMP, a link between the major second messenger cAMP
595 and the ability to pmf generation was proposed. The major contributor to pmf in *C. glutamicum* is
596 the cytochrome bc_1-aa_3 supercomplex and there is evidence from previous studies that expression
597 of the genes encoding the supercomplex is activated by the cAMP-dependent transcriptional
598 regulator GlxR. We observed reduced expression of the supercomplex genes and a reduced TMPD
599 oxidase activity in the Δ*cyaB* mutant, supporting the idea that a decreased supercomplex activity
600 contributes to the acetate sensitivity of the Δ*cyaB* mutant. Also the F_1F_O-ATP synthase genes are
601 known to be transcriptionally activated by GlxR and showed reduced expression in the Δ*cyaB*
602 mutant, additionally contributing to the energetic deficiencies of the strain. We could rescue the
603 growth defect of the Δ*cyaB* mutant on acetate by a single point mutation (A131T) in GlxR,
604 confirming the key role of GlxR for the phenotype of the Δ*cyaB* mutant. Additional studies are
605 required to elucidate the functional consequences of this amino acid exchange *in vivo*. In summary,
606 our results disclosed that cAMP in concert with GlxR plays a key role in the control of energy
607 metabolism in *C. glutamicum*.
608

CONFLICT OF INTEREST

The authors declare that the research was conducted in the absence of any commercial or financial relationships that could be construed as a potential conflict of interest.

AUTHOR CONTRIBUTIONS

NW and MBu constructed mutants and plasmids and performed all experimental work except the one specified below for other authors. AKK performed the analysis of glucose and organic acids. NK and JS performed the growth experiments with the protonophore CCCP and the determination of the membrane potential. TP supervised genome resequencing and analyzed the resulting data. JH and JAV performed LC-MS/MS measurements for cAMP determination. MBa coached the experimental work and supported the design of the study. All authors contributed to the interpretation of the data. NW wrote the first draft of the manuscript and prepared the figures and tables. MBo designed the study, supervised the experimental work, and wrote the final version of the manuscript.

SUPPLEMENTARY MATERIAL

Tables S1 and S2

Figs. S1 – S4

REFERENCES

Ammerman, J.W., and Azam, F. (1982). Uptake of cyclic AMP by natural populations of marine bacteria. *Appl. Environ. Microbiol.* 43**,** 869-876.

Arndt, A., Auchter, M., Ishige, T., Wendisch, V.F., and Eikmanns, B.J. (2008). Ethanol catabolism in *Corynebacterium glutamicum*. *J. Mol. Microbiol. Biotechnol.* 15(4)**,** 222-233.

Arndt, A., and Eikmanns, B.J. (2007). The alcohol dehydrogenase gene *adhA* in *Corynebacterium glutamicum* is subject to carbon catabolite repression. *J. Bacteriol.* 189**,** 7408-7416. doi: 10.1128/JB.00791-07.

Axe, D.D., and Bailey, J.E. (1995). Transport of lactate and acetate through the energized cytoplasmic membrane of *Escherichia coli*. *Biotechnol. Bioeng.* 47(1)**,** 8-19. doi: 10.1002/bit.260470103.

Becker, J., and Wittmann, C. (2012). Bio-based production of chemicals, materials and fuels - *Corynebacterium glutamicum* as versatile cell factory. *Curr. Opin. Biotechnol.* 23(4)**,** 631-640. doi: 10.1016/j.copbio.2011.11.012.

Binder, S., Schendzielorz, G., Stäbler, N., Krumbach, K., Hoffmann, K., Bott, M., et al. (2012). A high-throughput approach to identify genomic variants of bacterial metabolite producers at the single-cell level. *Genome Biol.* 13(5)**,** R40. doi: Doi 10.1186/Gb-2012-13-5-R40.

Bott, M. (2007). Offering surprises: TCA cycle regulation in *Corynebacterium glutamicum*. *Trends Microbiol.* 15(9)**,** 417-425.

Bott, M., and Niebisch, A. (2003). The respiratory chain of *Corynebacterium glutamicum*. *J. Biotechnol.* 104**,** 129-153.

Brazma, A., Hingamp, P., Quackenbush, J., Sherlock, G., Spellman, P., Stoeckert, C., et al. (2001). Minimum information about a microarray experiment (MIAME)-toward standards for microarray data. *Nat. Genet.* 29(4)**,** 365-371.

Burkovski, A. (ed.). (2008). *Corynebacteria: genomics and molecular biology.* Norfolk, U.K.: Caister Academic Press.

Bussmann, M., Emer, D., Hasenbein, S., Degraf, S., Eikmanns, B.J., and Bott, M. (2009). Transcriptional control of the succinate dehydrogenase operon *sdhCAB* of *Corynebacterium glutamicum* by the cAMP-dependent regulator GlxR and the LuxR-type regulator RamA. *J. Biotechnol.* 143(3)**,** 173-182.

Cha, P.H., Park, S.Y., Moon, M.W., Subhadra, B., Oh, T.K., Kim, E., et al. (2010). Characterization of an adenylate cyclase gene (*cyaB*) deletion mutant of *Corynebacterium glutamicum* ATCC 13032. *Appl. Microbiol. Biotechnol.* 85**,** 1061-1068.

da Luz, J.A., Hans, E., Frank, D., and Zeng, A.-P. (2016). Analysis of intracellular metabolites of *Corynebacterium glutamicum* at high cell density with automated sampling and filtration and assessment of engineered enzymes for effective L-lysine production. *Eng. Life Sci.* 17**,** 512-522.

Eggeling, L., and Bott, M. (eds.). (2005). *Handbook of Corynebacterium glutamicum.* Boca Raton, Florida, USA: CRC Press, Taylor & Francis Group.

Eggeling, L., and Bott, M. (2015). A giant market and a powerful metabolism: L-lysine provided by *Corynebacterium glutamicum*. *Appl. Microbiol. Biotechnol.* 99(8)**,** 3387-3394. doi: 10.1007/s00253-015-6508-2.

Eggeling, L., Bott, M., and Marienhagen, J. (2015). Novel screening methods-biosensors. *Curr. Opin. Biotechnol.* 35**,** 30-36. doi: 10.1016/j.copbio.2014.12.021.

Follmann, M., Ochrombel, I., Krämer, R., Trotschel, C., Poetsch, A., Rückert, C., et al. (2009). Functional genomics of pH homeostasis in *Corynebacterium glutamicum* revealed novel links between pH response, oxidative stress, iron homeostasis and methionine synthesis. *BMC Genomics* 10**,** 621. doi: 10.1186/1471-2164-10-621.

Frendorf, P.O., Lauritsen, I., Sekowska, A., Danchin, A., and Norholm, M.H.H. (2019). Mutations in the global transcription factor CRP/CAP: Insights from experimental evolution and deep sequencing. *Comput. Struct. Biotechnol. J.* 17**,** 730-736. doi: 10.1016/j.csbj.2019.05.009.

Freudl, R. (2017). Beyond amino acids: use of the *Corynebacterium glutamicum* cell factory for the secretion of heterologous proteins. *J. Biotechnol.* 258**,** 101-109. doi: 10.1016/j.jbiotec.2017.02.023.

Frunzke, J., Engels, V., Hasenbein, S., Gätgens, C., and Bott, M. (2008). Co-ordinated regulation of gluconate catabolism and glucose uptake in *Corynebacterium glutamicum* by two functionally equivalent transcriptional regulators, GntR1 and GntR2. *Mol. Microbiol.* 67(2)**,** 305-322.

Gerstmeir, R., Wendisch, V.F., Schnicke, S., Ruan, H., Farwick, M., Reinscheid, D., et al. (2003). Acetate metabolism and its regulation in *Corynebacterium glutamicum*. *J. Biotechnol.* 104(1-3)**,** 99-122.

Goldenbaum, P.E., and Hall, G.A. (1979). Transport of cyclic adenosine 3',5'-monophosphate across **Escherichia coli** vesicle membranes. *J. Bacteriol.* 140**,** 459-467.

Hartl, J., Kiefer, P., Meyer, F., and Vorholt, J.A. (2017). Longevity of major coenzymes allows minimal *de novo* synthesis in microorganisms. *Nat. Microbiol.* 2**,** 17073. doi: 10.1038/nmicrobiol.2017.73.

Heytler, P.G., and Prichard, W.W. (1962). A new class of uncoupling agents - carbonyl cyanide phenylhydrazones. *Biochem. Biophys. Res. Commun.* 7**,** 272-275. doi: 10.1016/0006-291x(62)90189-4.

ICH (2005). "Harmonised Tripartite Guideline, Validation of Analytical Procedures: Text and Methodology Q2 (R1)", in: *International Conference on Harmonisation of Technical Requirements for Registration of Pharmaceuticals for Human Use.*).

Ikeda, M., and Nakagawa, S. (2003). The *Corynebacterium glutamicum* genome: features and impacts on biotechnological processes. *Appl. Microbiol. Biotechnol.* 62(2-3)**,** 99-109.

Jolkver, E., Emer, D., Ballan, S., Krämer, R., Eikmanns, B.J., and Marin, K. (2009). Identification and characterization of a bacterial transport system for the uptake of pyruvate, propionate, and acetate in *Corynebacterium glutamicum*. *J. Bacteriol.* 191(3)**,** 940-948.

Jungwirth, B., Sala, C., Kohl, T.A., Uplekar, S., Baumbach, J., Cole, S.T., et al. (2013). High-resolution detection of DNA binding sites of the global transcriptional regulator GlxR in *Corynebacterium glutamicum*. *Microbiology* 159**,** 12-22. doi: 10.1099/mic.0.062059-0.

Kabashima, Y., Kishikawa, J., Kurokawa, T., and Sakamoto, J. (2009). Correlation between proton translocation and growth: Genetic analysis of the respiratory chain of *Corynebacterium glutamicum*. *J. Biochem.* 146(6)**,** 845-855.

Kabus, A., Niebisch, A., and Bott, M. (2007). Role of cytochrome *bd* oxidase from *Corynebacterium glutamicum* in growth and lysine production. *Appl. Environ. Microbiol.* 73**,** 861-868.

Kalinowski, J., Bathe, B., Bartels, D., Bischoff, N., Bott, M., Burkovski, A., et al. (2003). The complete *Corynebacterium glutamicum* ATCC 13032 genome sequence and its impact on the production of L-aspartate-derived amino acids and vitamins. *J. Biotechnol.* 104(1-3)**,** 5-25.

Kensy, F., Zang, E., Faulhammer, C., Tan, R.K., and Büchs, J. (2009). Validation of a high-throughput fermentation system based on online monitoring of biomass and fluorescence in continuously shaken microtiter plates. *Microb. Cell Fact.* 8**,** 31. doi: 10.1186/1475-2859-8-31.

Kim, H.J., Kim, T.H., Kim, Y., and Lee, H.S. (2004). Identification and characterization of *glxR*, a gene involved in regulation of glyoxylate bypass in *Corynebacterium glutamicum*. *J. Bacteriol.* 186(11)**,** 3453-3460.

Kinoshita, S., Udaka, S., and Shimono, M. (1957). Studies on amino acid fermentation. Part I. Production of L-glutamic acid by various microorganisms. *J. Gen. Appl. Microbiol.* 3**,** 193-205.

Koch-Koerfges, A., Kabus, A., Ochrombel, I., Marin, K., and Bott, M. (2012). Physiology and global gene expression of a *Corynebacterium glutamicum* ΔF_1F_O-ATP synthase mutant devoid of oxidative phosphorylation. *Biochim. Biophys. Acta* 1817(2)**,** 370-380. doi: S0005-2728(11)00238-6 [pii]

10.1016/j.bbabio.2011.10.006.

Koch-Koerfges, A., Pfelzer, N., Platzen, L., Oldiges, M., and Bott, M. (2013). Conversion of *Corynebacterium glutamicum* from an aerobic respiring to an aerobic fermenting bacterium by inactivation of the respiratory chain. *Biochim. Biophys. Acta* 1827(6)**,** 699-708. doi: 10.1016/j.bbabio.2013.02.004.

Kohl, T.A., Baumbach, J., Jungwirth, B., Pühler, A., and Tauch, A. (2008). The GlxR regulon of the amino acid producer *Corynebacterium glutamicum*: *In silico* and *in vitro* detection of DNA binding sites of a global transcription regulator. *J. Biotechnol.* 135(4)**,** 340-350.

Linder, J.U., Hammer, A., and Schultz, J.E. (2004). The effect of HAMP domains on class IIIb adenylyl cyclases from *Mycobacterium tuberculosis*. *Eur. J. Biochem.* 271(12)**,** 2446-2451. doi: 10.1111/j.1432-1033.2004.04172.x.

Möker, N., Brocker, M., Schaffer, S., Krämer, R., Morbach, S., and Bott, M. (2004). Deletion of the genes encoding the MtrA-MtrB two-component system of *Corynebacterium glutamicum* has a strong influence on cell morphology, antibiotics susceptibility and expression of genes involved in osmoprotection. *Mol. Microbiol.* 54(2)**,** 420-438.

Müller, J.E., Meyer, F., Litsanov, B., Kiefer, P., and Vorholt, J.A. (2015). Core pathways operating during methylotrophy of *Bacillus methanolicus* MGA3 and induction of a bacillithiol-dependent detoxification pathway upon formaldehyde stress. *Mol. Microbiol.* 98(6)**,** 1089-1100. doi: 10.1111/mmi.13200.

Mustafi, N., Grünberger, A., Kohlheyer, D., Bott, M., and Frunzke, J. (2012). The development and application of a single-cell biosensor for the detection of L-methionine and branched-chain amino acids. *Metab. Eng.* 14(4)**,** 449-457. doi: DOI 10.1016/j.ymben.2012.02.002.

Neumeyer, A., Hübschmann, T., Müller, S., and Frunzke, J. (2013). Monitoring of population dynamics of *Corynebacterium glutamicum* by multiparameter flow cytometry. *Microb. Biotechnol.* 6(2)**,** 157-167. doi: 10.1111/1751-7915.12018.

Nicholls, D.G., and Ferguson, S.J. (2002). *Bioenergetics 3.* London: Academic Press.

Niebisch, A., and Bott, M. (2001). Molecular analysis of the cytochrome bc_1-aa_3 branch of the *Corynebacterium glutamicum* respiratory chain containing an unusual diheme cytochrome c_1. *Arch. Microbiol.* 175(4)**,** 282-294.

Niebisch, A., and Bott, M. (2003). Purification of a cytochrome bc_1-aa_3 supercomplex with quinol oxidase activity from *Corynebacterium glutamicum* - Identification of a fourth subunit of cytochrome aa_3 oxidase and mutational analysis of diheme cytochrome c_1. *J. Biol. Chem.* 278(6)**,** 4339-4346.

Novo, D., Perlmutter, N.G., Hunt, R.H., and Shapiro, H.M. (1999). Accurate flow cytometric membrane potential measurement in bacteria using diethyloxacarbocyanine and a ratiometric technique. *Cytometry* 35(1)**,** 55-63.

Novo, D.J., Perlmutter, N.G., Hunt, R.H., and Shapiro, H.M. (2000). Multiparameter flow cytometric analysis of antibiotic effects on membrane potential, membrane permeability, and bacterial counts of Staphylococcus aureus and Micrococcus luteus. *Antimicrob. Agents Chemother.* 44(4)**,** 827-834. doi: 10.1128/aac.44.4.827-834.2000.

Pfeifer-Sancar, K., Mentz, A., Rückert, C., and Kalinowski, J. (2013). Comprehensive analysis of the *Corynebacterium glutamicum* transcriptome using an improved RNAseq technique. *BMC Genomics* 14**,** 888. doi: 10.1186/1471-2164-14-888.

Pinhal, S., Ropers, D., Geiselmann, J., and de Jong, H. (2019). Acetate metabolism and the inhibition of bacterial growth by acetate. *J. Bacteriol.* 201(13). doi: 10.1128/JB.00147-19.

Polen, T., and Wendisch, V.F. (2004). Genomewide expression analysis in amino acid-producing bacteria using DNA microarrays. *Appl. Biochem. Biotechnol.* 118(1-3)**,** 215-232. doi: 10.1385/abab:118:1-3:215.

Richter, W. (2002). 3',5' Cyclic nucleotide phosphodiesterases class III: members, structure, and catalytic mechanism. *Proteins* 46**,** 278-286.

784 Saier, M.H., Jr., Feucht, B.U., and McCaman, M.T. (1975). Regulation of intracellular adenosine
785 cyclic 3':5'-monophosphate levels in *Escherichia coli* and *Salmonella typhimurium*.
786 Evidence for energy-dependent excretion of the cyclic nucleotide. *J. Biol. Chem.* 250(19)**,**
787 7593-7601.

788 Sakamoto, J., Shibata, T., Mine, T., Miyahara, R., Torigoe, T., Noguchi, S., et al. (2001).
789 Cytochrome *c* oxidase contains an extra charged amino acid cluster in a new type of
790 respiratory chain in the amino-acid-producing Gram-positive bacterium *Corynebacterium*
791 *glutamicum*. *Microbiology* 147**,** 2865-2871.

792 Sambrook, J., and Russell, D. (2001). *Molecular Cloning. A Laboratory Manual.* Cold Spring
793 Harbor, New York: Cold Spring Harbor Laboratory Press.

794 Schäfer, A., Tauch, A., Jäger, W., Kalinowski, J., Thierbach, G., and Pühler, A. (1994). Small
795 mobilizable multipurpose cloning vectors derived from the *Escherichia coli* plasmids pK18
796 and pK19 - Selection of defined deletions in the chromosome of *Corynebacterium*
797 *glutamicum*. *Gene* 145(1)**,** 69-73.

798 Schendzielorz, G., Dippong, M., Grünberger, A., Kohlheyer, D., Yoshida, A., Binder, S., et al.
799 (2014). Taking control over control: Use of product sensing in single cells to remove flux
800 control at key enzymes in biosynthesis pathways. *ACS Synth. Biol.* 3**,** 21-29. doi:
801 10.1021/sb400059y.

802 Schneider, J., and Wendisch, V.F. (2011). Biotechnological production of polyamines by bacteria:
803 recent achievements and future perspectives. *Appl. Microbiol. Biotechnol.* 91(1)**,** 17-30.

804 Schulte, J., Baumgart, M., and Bott, M. (2017a). Development of a single-cell GlxR-based cAMP
805 biosensor for *Corynebacterium glutamicum*. *J. Biotechnol.* 258**,** 33-40. doi:
806 10.1016/j.jbiotec.2017.07.004.

807 Schulte, J., Baumgart, M., and Bott, M. (2017b). Identification of the cAMP phosphodiesterase
808 CpdA as novel key player in cAMP-dependent regulation in *Corynebacterium glutamicum*.
809 *Mol. Microbiol.* 103**,** 534-552. doi: 10.1111/mmi.13574.

810 Shenoy, A.R., Sivakumar, K., Krupa, A., Srinivasan, N., and Visweswariah, S.S. (2004). A
811 survey of nucleotide cyclases in Actinobacteria: unique domain organization and expansion
812 of the class III cyclase family in *Mycobacterium tuberculosis*. *Comp. Funct. Genomics* 5**,**
813 17-38.

814 Studier, F.W. (2005). Protein production by auto-induction in high density shaking cultures.
815 *Protein Expr. Purif.* 41(1)**,** 207-234. doi: 10.1016/j.pep.2005.01.016.

816 Studier, F.W., and Moffatt, B.A. (1986). Use of bacteriophage T7 RNA polymerase to direct
817 selective high-level expression of cloned genes. *J. Mol. Biol.* 189**,** 113-130.

818 Townsend, P.D., Jungwirth, B., Pojer, F., Bussmann, M., Money, V.A., Cole, S.T., et al. (2014).
819 The crystal structures of apo and cAMP-bound GlxR from *Corynebacterium glutamicum*
820 reveal structural and dynamic changes upon cAMP binding in CRP/FNR family
821 transcription factors. *PLoS One* 9(12)**,** e113265. doi: 10.1371/journal.pone.0113265.

822 Toyoda, K., Teramoto, H., Inui, M., and Yukawa, H. (2011). Genome-wide identification of *in*
823 *vivo* binding sites of GlxR, a cyclic AMP receptor protein-type regulator in
824 *Corynebacterium glutamicum*. *J. Bacteriol.* 193**,** 4123-4133. doi: 10.1128/JB.00384-11.

825 van Ooyen, J., Emer, D., Bussmann, M., Bott, M., Eikmanns, B.J., and Eggeling, L. (2011).
826 Citrate synthase in *Corynebacterium glutamicum* is encoded by two *gltA* transcripts which
827 are controlled by RamA, RamB, and GlxR. *J. Biotechnol.* 154**,** 140-148. doi:
828 doi:10.1016/j.jbiotec.2010.07.004.

829 Wendisch, V.F., De Graaf, A.A., Sahm, H., and Eikmanns, B.J. (2000). Quantitative
830 determination of metabolic fluxes during coutilization of two carbon sources: comparative
831 analyses with *Corynebacterium* glutamicum during growth on acetate and/or glucose. *J.*
832 *Bacteriol.* 182(11)**,** 3088-3096.

833 Wieschalka, S., Blombach, B., Bott, M., and Eikmanns, B.J. (2013). Bio-based production of
834 organic acids with *Corynebacterium glutamicum*. *Microb. Biotechnol.* 6(2)**,** 87-102. doi:
835 10.1111/1751-7915.12013.

836 Yukawa, H., and Inui, M. (eds.). (2013). *Corynebacterium glutamicum: Biology and*
837 *Biotechnology.* Heidelberg: Springer.

838 Yukawa, H., Omumasaba, C.A., Nonaka, H., Kos, P., Okai, N., Suzuki, N., et al. (2007).
839 Comparative analysis of the *Corynebacterium glutamicum* group and complete genome
840 sequence of strain R. *Microbiology* 153**,** 1042-1058.

841

TABLE 1 Bacterial strains and plasmids used in this study

Strain or plasmid	Relevant characteristics	Source or reference
Strains		
Escherichia coli DH5α	F⁻ *thi-1 endA1 hsdR17*(r-m+) *supE44* Δ*lacU169*Φ80*lacZ*Δ*M15*) *recA1 gyrA96 relA1*	Invitrogen
Escherichia coli BL21(DE3)		(Studier and Moffatt, 1986)
Corynebacterium glutamicum ATCC 13032	ATCC 13032, biotin-auxotrophic wild-type strain (WT)	(Kinoshita et al., 1957)
C. glutamicum Δ*cyaB*	ATCC 13032 with an in frame deletion of the adenylate cyclase gene *cyaB* (cg0375)	This study
C. glutamicum Δ*cpdA*	ATCC 13032 with an in frame deletion of the phosphodiesterase gene *cpdA* (cg2761)	(Schulte et al., 2017b)
C. glutamicum Δ*cyaB*Δ*cpdA*	ATCC 13032 with an in frame deletion of the gene *cyaB* and the phosphodiesterase gene *cpdA* (Δ*cyaB*Δ*cpdA*)	This study
C. glutamicum Δ*qcr*	ATCC 13032 with an in frame deletion of the *qcrCAB* genes encoding the three subunits of the bc_1 complex	(Niebisch and Bott, 2001)
C. glutamicum Δ*cyaB*_sup1	*C. glutamicum* Δ*cyaB* suppressor mutant carrying a single genomic mutation (C to T) at position 307072 in BA000036.3 leading to the amino acid exchange Ala131Thr in GlxR (cg0350)	This study
C. glutamicum Δ*cyaB*_sup2	*C. glutamicum* Δ*cyaB* suppressor mutant carrying two genomic mutations in BA000036.3, one at position 877553 (A to G) located in the intergenic region of *serC* (cg0948) and *gpt* (cg0949) and one at position 1548741 (G to C) located in the intergenic region of *gpt* (cg1659) and cg1660	This study

C. glutamicum Δ*cyaB*_sup3	*C. glutamicum* Δ*cyaB* suppressor mutant carrying two genomic mutations in BA000036.3, one at position 307072 (C to T) leading to the amino acid exchange Ala131Thr in GlxR and one at position 2564086 (G to T) leading to a silent mutation of the Gly106 codon of ribose 5-phosphate isomerase (cg2658)	This study
*C. glutamicum::glxR*_A131T	*C. glutamicum* WT in which an Ala131Thr exchange in the *glxR* coding sequence was introduced by double homologous recombination	This study
C. glutamicum Δ*cyaB::glxR*_A131T	*C. glutamicum* Δ*cyaB* mutant in which an Ala131Thr exchange in the *glxR* coding sequence was introduced by double homologous recombination	This study
Plasmids		
pAN6	Kan^R; P_{tac}, $lacI^q$ pBL1 $oriV_{Cg}$ pUC18 $oriV_{Ec}$, *C. glutamicum/E. coli* shuttle vector, derivative of pEKEx2	(Frunzke et al., 2008)
pAN6-*cyaB*	Kan^R; pAN6 derivative carrying the *cyaB* gene (cg0375) including 300 bp upstream of the start codon and a 3'-terminal StrepTag-II-encoding sequence under the control of an IPTG-inducible *tac* promoter	This study
pAN6-*glxR*-Twinstrep	Kan^R; pAN6 derivative carrying the *glxR* gene (cg0350) including a 3'-terminal Twinstrep-tag encoding sequence before the stop codon (WSHPQFEKGGGSGGGSGGSAWSHPQFEK)	This study
pAN6-*glxR*-A131T-Twinstrep	Kan^R; pAN6-glxR-Twinstrep derivative with a Ala131T exchange	This study
pK19*mobsacB*	Kan^R; oriT $oriV_{Ec}$ *sacB lacZα;* vector for allelic exchange in *C. glutamicum*	(Schäfer et al., 1994)
pK19*mobsacB*-Δ*cyaB*	Kan^R; pK19*mobsacB* derivative containing an overlap extension PCR product covering the up- and downstream regions of *cyaB*	This study

pK19*mobsacB*-Δ*cpdA*	Kan^R; pK19*mobsacB* derivative containing an overlap extension PCR product covering the up- and downstream regions of *cpdA*	(Schulte et al., 2017b)
pK19*mobsacB*-*glxR*_mut	Kan^R; pK19*mobsacB* derivative containing a 800-bp PCR product covering the 3'-terminal 684 bp of *glxR* including the mutation leading to the Ala131Thr exchange and 116 bp of the downstream region	This study

TABLE 2 cAMP levels in various *C. glutamicum* strains cultivated in CGXII medium with 100 mM glucose.

C. glutamicum strain	Intracellular cAMP concentration[1]	
	pmol mg^{-1} protein (determined by ELISA)	µM (determined by LC-MS/MS)
WT	99.9 ± 31.8	0.9 ± 0.4
Δ*cyaB*	20.5 ± 4	n.d.[2]
Δ*cpdA*	144.1 ± 7.9	3.4 ± 1.5
Δ*cyaB*Δ*cpdA*	30 ± 6.8	n.d.

[1] Each value represents the mean value with the standard deviation of three biological replicates.

[2] n.d., not detectable

FIGURE LEGENDS

FIGURE 1. Growth of *C. glutamicum* WT and the Δ*cyaB* mutant in CGXII medium with **(A)** 100 mM acetate, **(B)** 100 mM gluconate or gluconate-acetate mixture (100 mM each), (**C**) 100 mM glucose or glucose-acetate mixture (100 mM each), (**D**) 100 mM fructose or fructose-acetate mixture (100 mM each), and (**E**) 100 mM sucrose or sucrose-acetate mixture (100 mM each). Mean values and standard deviations of three biological replicates are shown.

FIGURE 2. Growth and substrate consumption of *C. glutamicum* WT and its Δ*cyaB* mutant in CGXII minimal medium containing either **(A)** glucose and acetate (100 mM each) or **(B)** gluconate and acetate (100 mM each). Panels **C** and **D** show the acetate consumption by the cultures displayed in panels A and B. Panel **E** shows the glucose consumption of the cultures displayed in panel A and panel **F** shows the gluconate consumption of the cultures displayed in panel B. The strains were cultivated at 30°C and 120 rpm in 500 ml baffled shake flasks containing 50 ml CGXII minimal medium with the depicted carbon source. Mean values and standard deviations of three biological replicates are shown.

FIGURE 3. Complementation of the Δ*cyaB* mutant with plasmid-encoded *cyaB* (pAN6-*cyaB*) or the addition of 10 mM extracellular cAMP (+ cAMP). The cultures contained 0.25 mM IPTG, 25 μg ml^{-1} kanamycin and, where indicated, 10 mM cAMP. Mean values and standard deviations of three biological replicates are shown.

FIGURE 4. Growth of *C. glutamicum* WT and the Δ*cyaB* mutant in CGXII medium with increasing sodium acetate concentrations (**A**). pH dependency of growth of *C. glutamicum* WT and the Δ*cyaB* mutant in modified CGXII medium containing 20 g l^{-1} MOPS and 20 g l^{-1} MES buffer (pH adjusted with either KOH or HCl) with either 100 mM glucose (**B**) or 100 mM acetate (**C**) as carbon source. Mean values and standard deviations of three biological replicates are shown.

FIGURE 5. Growth of *C. glutamicum* WT (**A**) and the Δ*cyaB* mutant (**B**) in CGXII medium with 2% (w/v) glucose in the presence of different CCCP concentrations. Mean values and standard deviations of three biological replicates are shown. (**C**) Relative comparison of the membrane potential (ΔΨ) of *C. glutamicum* cells by flow cytometry of (DiOC2(3))-stained cells. Overlays of the histograms obtained with WT cells and Δ*cyaB* mutant cells are shown. The percentage of analyzed cells (% of Max) is plotted versus the logarithm of the red/green fluorescence ratio. This ratio serves as an indicator of ΔΨ, with a high value corresponding to a high ΔΨ. Panel I shows a

control experiment with glucose-grown WT cells that were treated for 15 min without or with 50 µM CCCP to collapse ΔΨ. Panels II, III, and IV show comparisons of WT and Δ*cyaB* cells cultivated in CGXII medium with either 100 mM glucose (II), 100 mM acetate (III), or 200 mM acetate (IV). Representative histograms of three biological and three technical replicates each are shown. The histograms were generated with the software FlowJo V.10 and processed in GraphPad Prism8.

FIGURE 6. Growth of the indicated *C. glutamicum* strains in CGXII medium with either 100 mM glucose (**A**), 100 mM glucose plus 150 mM potassium acetate (**B**), or 150 mM potassium acetate as carbon source (**C**). Mean values and standard deviations of three biological replicates are shown.

frontiers

Supplementary Material

1 Supplementary Tables

TABLE S1. Oligonucleotides used in this study

Oligonucleotide	Sequence (5' → 3') and properties[1]
Construction of deletion plasmid pK19*mobsacB-cyaB* and PCR-analysis of the resulting mutants	
del0375_1_*Hind*III-fw	ATTAAAGCTTCGGGGTGGCTGCCTCCCATG
del0375_2-rv	CGTTTAGGTTTAGTGGCTGGGCAAACAGCATTACTGCGAGCGCACC
del0375_3-fw	CCCAGCCACTAAACCTCCCCGGCGGCCTATTCGGCCGACGTTG
del0375_4_*Xba*I-rv	ATTATCTAGACAATCACGCCGCGTACATCGC
cg0375_deltest-fw	CAATTGCTGCGGGACGATGTG
cg0375_deltest-rv	GATTCACTGCCTAAAGGTGCG
Construction of deletion plasmid pK19*mobsacB-cpdA* and PCR-analysis of the resulting mutants	
cg2761_deltest-fw	GCACAGTGGGAACCATTAAC
cg2761_deltest-rv	GTGGTCGTGATTGTACTTCC
Construction of plasmid pAN6-*cyaB* and sequencing of the insert	
pAN6-*cyaB*-Pst-fw	AAAACTGCAGATAGACAATTGCTGCGGG
pAN6-*cyaB*-NheI-rv	AAAAGCTAGCGGACCTATCCGCCAACGTC
pAN6_seq_fw	TTACGCCAAGCTTGCATG
pAN6_seq_rv	GTAAAACGACGGCCAGTG
Construction of WT::*glxR*$_{A131T}$ and Δ*cyaB*::*glxR*_A131T mutant and PCR analysis of the mutation	
cg0350_mut_A131T_fw	CCTGCAGGTCGACTCTAGAGTTCGTTACCTGCAGGCTCAGGAAGCTTC
cg0350_mut_A131T_rv	GTAAAACGACGGCCAGTGAATTGTGGAAGGTGTACAGGAGATCCTGTC
cg0350_mut_control	TCGAGCGCGACGTGCCAAATGC
Oligonucleotides for qRT-PCR analysis	
RT-*ctaD*-fw1	TGAACAGCTGGTTGAACTGC
RT-*ctaD*-rv1	TCCTTCAGCTTCTTCTTCCTCG
RT-*ctaC*-fw1	GCATTACCCCTGAAGCAGTG
RT-*ctaC*-rv1	ATGGCGGTGAGGAATAGACC
RT-*qcrC*-fw1	CTGCCACAACTTCACTGGTC
RT-*qcrC*-rv1	TAGGCATGTTCTGAGGACCG
RT_*hpt*_fw	ATGTTCCAGCCAACCCATAC
RT_*hpt*_rv	TCTTCGGCGTCTTTGAACTC
Oligonucleotides for plasmid pAN6-*glxR*-Twinstrep and pAN6-*glxR*_A131T-TwinStrep	
GlxR-twin1	GCCTGCAGAAGGAGATATACAGTGGAAGGTGTACAGGAG
GlxR-twin2	TCGAGCGCGACGTGCCAAATGC
GlxR-twin3	GGCACGTCGCGCTCGATGGAGTCATCCTCAATTCG
GlxR-twin4	AAACGACGGCCAGTGAATTTTATTTTTCGAACTGCGGGTG
GlxR-A131T_fw	TCCTGCGCGTTCTGACTCGTCGTCTGCGTCGC
GlxR-A131T_rv	GCGACGCAGACGACGAGTCAGAACGCGCAGGA
EMSA	
EMSA_*ctaC*_fw	GGTGGAAATATCTTCGTGGGTTTCG
EMSA_*ctaC*_rv	GTTGATGGTCTGTGACGTGG
EMSA_*ctaD*_fw	CTGTATCCCCTTTTCATGC
EMSA_*ctaD*_rv	CTTCCTGGCGAAATGTCCG
EMSA_neg _fw	AGCTGCTGCGTTCAGGTGTC
EMSA_neg_rv	TAGTGGCGGTGGATCAGG

[1]Restriction sites are underlined

TABLE S2. mRNA ratios (Δ*cyaB*/WT) of the genes encoding F_1F_O-ATP synthase and the cytochrome bc_1-aa_3 supercomplex.[1]

Locus tag	Gene	Function	mRNA ratio Δ*cyaB*/WT	
			DNA microarrays[2]	qRT-PCR[3]
cg1362	*atpB*	ATP synthase subunit A	0.51	n.d.[4]
cg1363	*atpE*	ATP synthase subunit C	0.51[5]	n.d.
cg1364	*atpF*	ATP synthase subunit B	0.53	n.d.
cg1365	*atpH*	ATP synthase subunit δ	0.55	n.d.
cg1366	*atpA*	ATP synthase subunit α	0.41	n.d.
cg1367	*atpG*	ATP synthase subunit γ	0.40	n.d.
cg1368	*atpD*	ATP synthase subunit β	0.43	n.d.
cg1369	*atpC*	ATP synthase subunit ε	0.83	n.d.
cg2406	*ctaE*	cytochrome aa_3 oxidase subunit 3	0.67	n.d.
cg2409	*ctaC*	cytochrome aa_3 oxidase subunit 2	0.63	0.20
cg2408	*ctaF*	cytochrome aa_3 oxidase subunit 4	0.31	n.d.
cg2780	*ctaD*	cytochrome aa_3 oxidase subunit 1	0.69	0.32
cg2405	*qcrC*	cytochrome c_1	0.74	0.30
cg2404	*qcrA*	Rieske iron-sulfur protein	0.64	n.d.
cg2403	*qcrB*	cytochrome *b*	0.64	n.d.

[1]Cells of the Δ*cyaB* mutant and the WT were grown in CGXII medium with glucose plus acetate (100 mM each).
[2]mRNA ratios represent mean values of at least two DNA microarray analyses starting from independent cultures.
[3]qRT-PCR results represent mean values of three biological replicates and two technical replicates each
[4]n.d., not determined
[5]except for cg1363, the p-values for all other genes were ≤0.05

2 Supplementary Figures

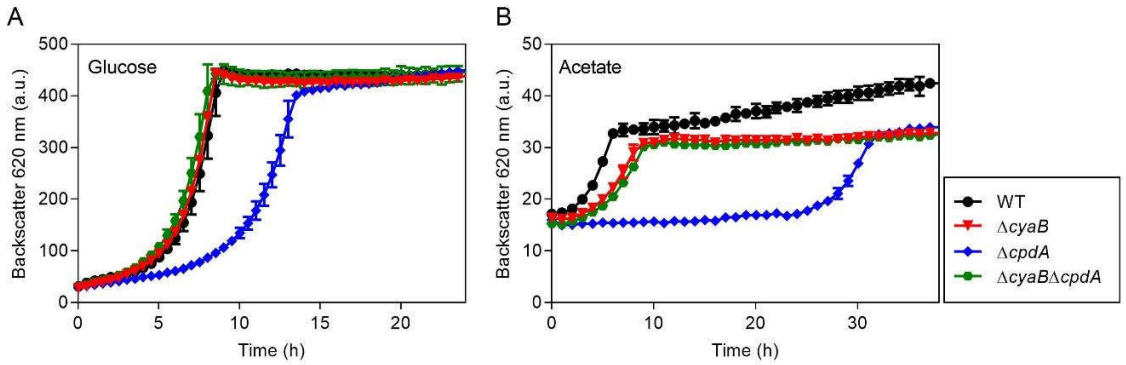

FIGURE S1. Growth of *C. glutamicum* WT and the mutant strains Δ*cyaB*, Δ*cpdA*, and Δ*cyaB*Δ*cpdA* in CGXII medium with 2% (w/v) glucose (**A**) or 100 mM sodium acetate (**B**). Mean values and standard deviations of three biological replicates are shown.

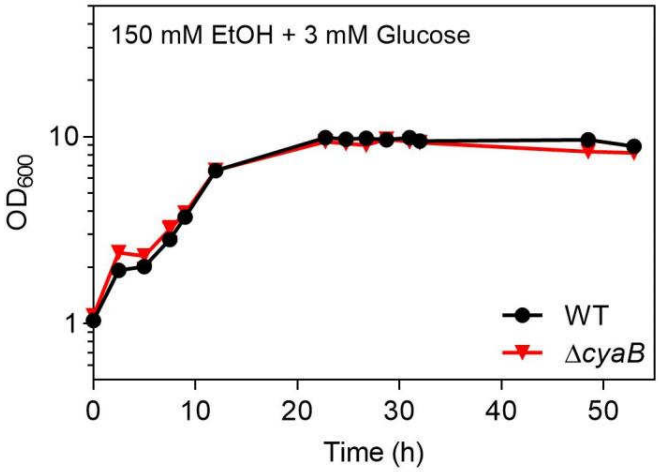

FIGURE S2. Growth of *C. glutamicum* WT and the Δ*cyaB* mutant in CGXII minimal medium with 150 mM ethanol and 3 mM glucose. Cultivation was performed in baffled shake flasks that were incubated at 30 °C and 120 rpm at 85% humidity. Mean values and standard deviations of three biological replicates are shown.

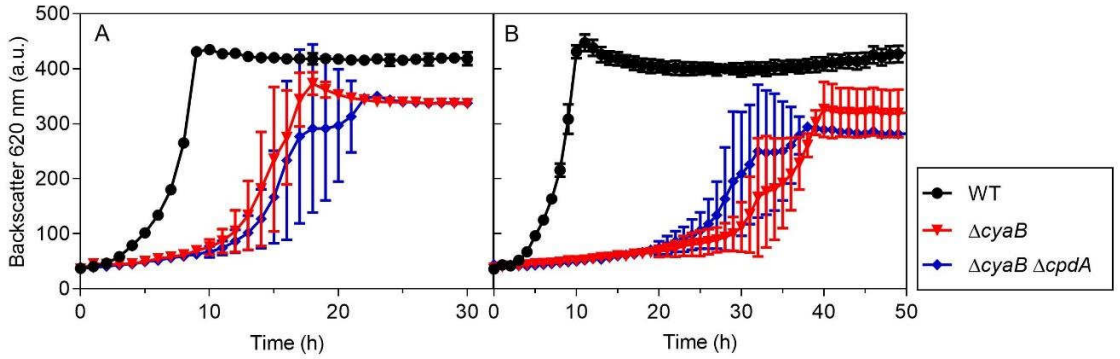

FIGURE S3. Growth of *C. glutamicum* WT and mutant strains Δ*cyaB* and Δ*cyaB*Δ*cpdA* in CGXII medium with 100 mM glucose and 50 mM potassium acetate (**A**) or with 100 mM glucose and 100 mM potassium acetate (**B**). Mean values and standard deviations of three biological replicates are shown.

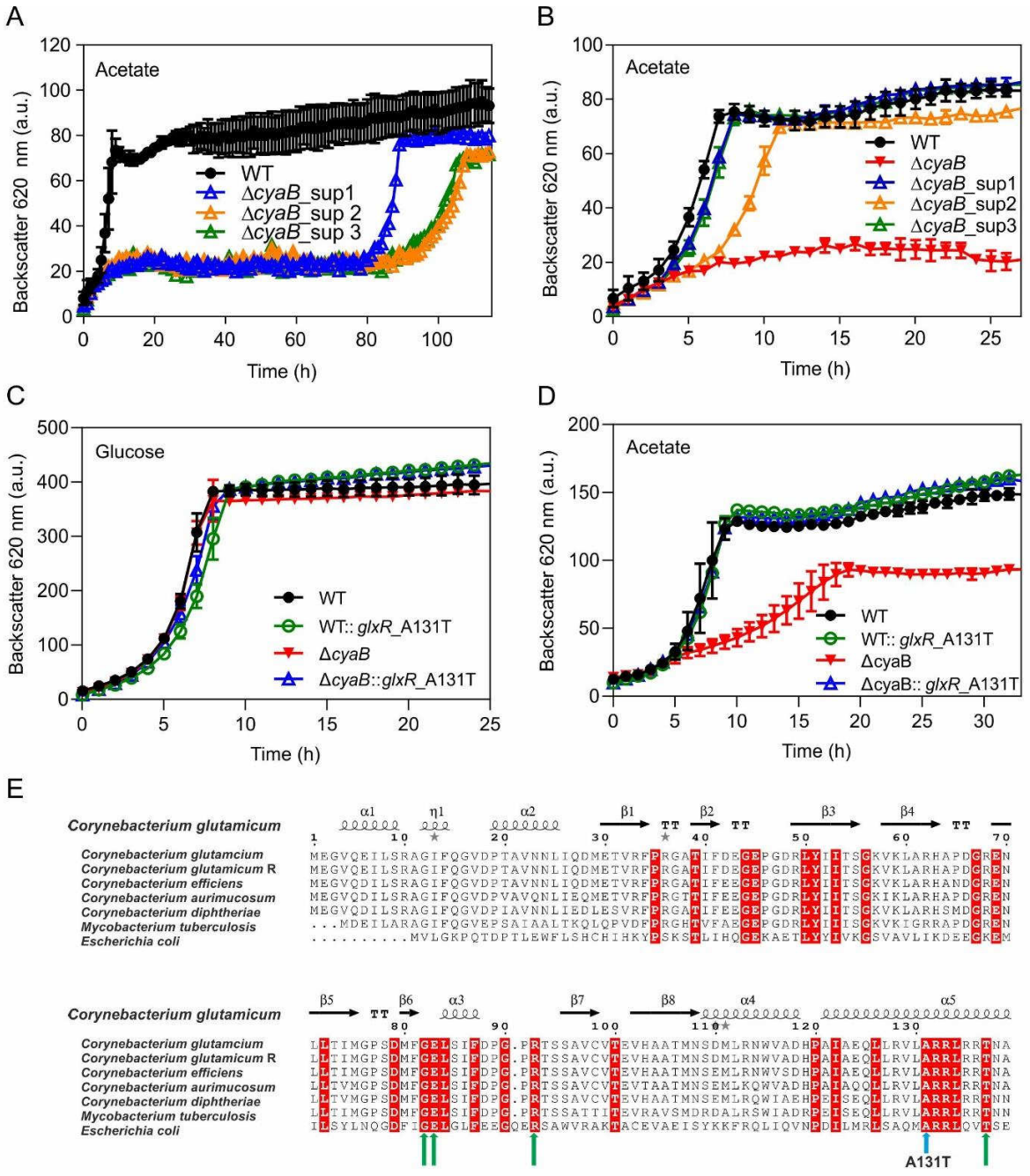
A
Acetate
Backscatter 620 nm (a.u.)
Time (h)
WT
ΔcyaB_sup1
ΔcyaB_sup 2
ΔcyaB_sup 3
B
Acetate
Backscatter 620 nm (a.u.)
Time (h)
WT
ΔcyaB
ΔcyaB_sup1
ΔcyaB_sup2
ΔcyaB_sup3
C
Glucose
Backscatter 620 nm (a.u.)
Time (h)
WT
WT:: glxR_A131T
ΔcyaB
ΔcyaB::glxR_A131T
D
Acetate
Backscatter 620 nm (a.u.)
Time (h)
WT
WT:: glxR_A131T
ΔcyaB
ΔcyaB:: glxR_A131T
E
Corynebacterium glutamicum
Corynebacterium glutamcium
Corynebacterium glutamicum R
Corynebacterium efficiens
Corynebacterium aurimucosum
Corynebacterium diphtheriae
Mycobacterium tuberculosis
Escherichia coli
A131T
F
G

FIGURE S4. (A) Generation of suppressor mutants of *C. glutamicum* Δ*cyaB* with restored growth on acetate in a long-term cultivation in CGXII medium with 150 mM potassium acetate. **(B)** Growth of single colonies of the Δ*cyaB* suppressor mutant in CGXII medium with 150 mM acetate using *C. glutamicum* WT and the Δ*cyaB* mutant as controls. **(C, D)** Growth of indicated strains in CGXII medium with 100 mM glucose or 100 mM acetate. The *glxR*_A131T mutation identified in the Δ*cyaB* suppressor mutant was introduced by homologous recombination into the genomes of the WT and the Δ*cyaB* mutant. **(E)** Section of an amino acid sequence alignment of GlxR homologs from different bacterial strains. GlxR (Cg0350) of *C. glutamicum* WT and features derived from its crystal structure (PDB 4CYD) were used as reference. Red boxed amino acids are conserved in all selected sequences. Green arrows indicate residues important for cAMP binding in GlxR according to structural analysis (Townsend et al., 2014). The blue arrow shows the position of the A131T exchange in the Δ*cyaB*_sup1 mutant. The alignment was performed with Clustal W (https://www.genome.jp/tools-bin/clustalw) and processed with ESPript 3 (Robert and Gouet, 2014). The following sequences were used for the alignment: *C. glutamicum* strain R CgR0377; *Corynebacterium efficiens* YS-314 CE0287; C*orynebacterium aurimucosum* ATCC700975 Cauri0205; *Corynebacterium diphtheriae* NCTTC13129 CDIP0303; *Mycobacterium tuberculosis* H37Rv Rv3676; *Escherichia coli* MG1655 b3357. (**F**) Overlay of apo-$GlxR_{WT}$ (green) (PDB:4BYY) and model of apo-$GlxR_{A131T}$ (light blue). (**G**) Overlay of holo-$GlxR_{WT}$ (green) (PDB:4CYD) and a model of holo-$GlxR_{A131T}$ (light blue) showing an enlargement of the region close to A131T amino acid exchange including bound cAMP. The model of GlxR-A131T and the overlay were generated with PyMOL.

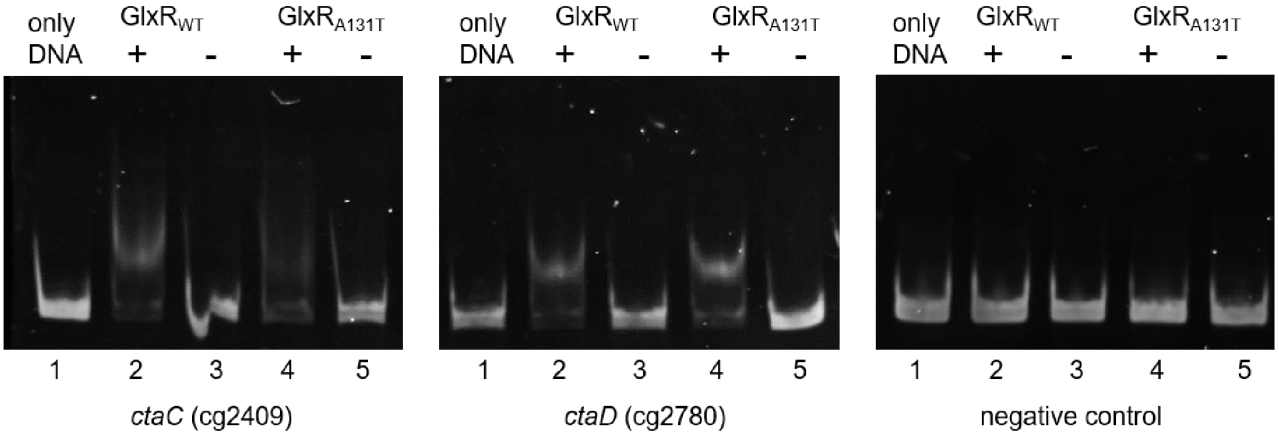

FIGURE S5. Electrophoretic mobility shift assays (EMSAs) with C-terminally Twin-Streptagged GlxR$_{WT}$ or GlxR$_{A131T}$ and DNA fragments covering the known GlxR-binding sites in the promoter regions of *ctaD* (-121 to -261 bp upstream of *ctaD* start codon) and *ctaCF* (-102 to -234 bp upstream of *ctaC* start codon) (Kohl et al., 2008; Toyoda et al., 2011) and an intragenic DNA fragment of cg3153 serving as negative control. 100 ng of the DNA fragments were incubated for 30 min at room temperature with 200 nM purified protein, either with (+) or without (-) 0.2 mM cAMP. After incubation, the reaction mixture was loaded on a 10% native polyacrylamide gel. Lane 1: control sample containing only DNA; lane 2: sample with GlxR$_{WT,\ the}$ indicated DNA fragment, and cAMP; lane 3: sample with GlxR$_{WT}$ and the indicated DNA fragment, but without cAMP; lane 4: sample of GlxR$_{A131T}$ with the indicated DNA fragment and cAMP; lane 5: sample with GlxR$_{A131T}$ and the indicated DNA fragment, but without cAMP.

3 Supplementary References

Kohl, T.A., Baumbach, J., Jungwirth, B., Pühler, A., and Tauch, A. (2008). The GlxR regulon of the amino acid producer *Corynebacterium glutamicum*: *In silico* and *in vitro* detection of DNA binding sites of a global transcription regulator. *J. Biotechnol.* 135(4), 340-350.

Robert, X., and Gouet, P. (2014). Deciphering key features in protein structures with the new ENDscript server. *Nucleic Acids Res.* 42, W320-324. doi: 10.1093/nar/gku316.

Townsend, P.D., Jungwirth, B., Pojer, F., Bussmann, M., Money, V.A., Cole, S.T., et al. (2014). The crystal structures of apo and cAMP-bound GlxR from *Corynebacterium glutamicum* reveal structural and dynamic changes upon cAMP binding in CRP/FNR family transcription factors. *PLoS One* 9(12), e113265. doi: 10.1371/journal.pone.0113265.

Toyoda, K., Teramoto, H., Inui, M., and Yukawa, H. (2011). Genome-wide identification of *in vivo* binding sites of GlxR, a cyclic AMP receptor protein-type regulator in *Corynebacterium glutamicum*. *J. Bacteriol.* 193, 4123-4133. doi: 10.1128/JB.00384-11.